JOURNAL OF SOLID STATE CHEMISTRY 92, 386–400 (1991)

Synthesis, Structure, and Properties of a New T* Structure Copper-Oxychloride of $MLnCuO_3Cl$ (M = Ca, Sr and Ln = Nd, Sm, Eu, Gd)

ROBERT L. FULLER AND MARTHA GREENBLATT*

Rutgers, The State University of New Jersey, Piscataway, New Jersey 08855

Received October 12, 1990; in revised form February 6, 1991

The syntheses of a new copper oxychloride with the general formula of $MLnCuO_3Cl$ (M = Ca, Sr and Ln =Nd, Sm, Eu, Gd) are reported. These compounds are shown to have the T* structure where the copper atoms are coordinated by a square pyramidal geometry with a chloride ion in the apical position. This structure is supported by the X-ray powder patterns and lattice parameters of the new oxychlorides. The substitution of Sr for Ca in $Ca_{1-x}Sr_xLnCuO_3Cl$ with Ln = Nd, Sm was performed, and the substitution is discussed in terms of the size requirements of the T* structure. Alternating current impedance measurements for $CaSmCuO_3Cl$ and $Ca_{0.72}Sr_{0.28}NdCuO_3Cl$ from 100 to 600°C are presented; when annealed in oxygen, $CaSmCuO_3Cl$ showed semiconducting behavior with an activation energy of 0.12 eV. When these two samples were annealed in argon, ionic conductivity from oxygen vacancies was observed. Magnetic susceptibility measurements for $CaSmCuO_3Cl$ and $Ca_{0.72}Sr_{0.28}NdCuO_3Cl$ from 2 to 400 K show similarity to the magnetic results for Sm_2CuO_4 and Nd_2CuO_4, respectively. The resistivity and magnetic measurements indicate that the properties of these compounds are similar to those of their parent copper oxides, Ln_2CuO_4, and not to their parent oxychlorides, $M_2CuO_2Cl_2$ (M = Ca, Sr).

1. Introduction

With the initial discovery of superconductivity in $La_{2-x}Sr_xCuO_4$, several copper oxides have been found to superconduct at relatively high temperatures. This new class of materials has two basic characteristics. First, they all contain a copper–oxygen plane where the charge carriers are primarily located, and second, a metal-oxide layer that is located between the copper–oxygen planes. This oxide layer is essential as a charge reservoir to allow charge carriers to be doped into the copper–oxygen plane. The stacking of these two layers gives rise to several possible forms of coordination about the copper. In compounds such as $La_{2-x}Sr_xCuO_4$, the copper is surrounded by an octahedron of oxide ions; in $YBa_2Cu_3O_7$ and $Nd_{1.32}Sr_{0.41}Ce_{0.27}CuO_{4-y}$, the copper is surrounded by a square pyramid of oxide ions (*1*). For these two classes of superconductors, the predominant charge carriers are holes. Another class of copper oxides which are known to superconduct are those with the T′ structure (such as $Nd_{2-x}Ce_xCuO_4$) (*2*). In these compounds, the metal-oxide layer has a distorted fluorite structure, yielding a square planar coordination of the copper. The charge carriers in these compounds are primarily electrons (*3*, *4*).

If the metal-oxide layer was simply a charge reservoir, then it could be composed of any material that could dope the appro-

* To whom correspondence should be addressed.

0022-4596/91 $3.00

priate charge carriers into the copper–oxygen plane and, in turn, induce superconductivity. To date, all of the high temperature superconductors have been substituted copper oxides (with the exception of (Ba,K) BiO_3); however, a class of copper oxychlorides shows potential. In particular, $Sr_2CuO_2Cl_2$ and $Ca_2CuO_2Cl_2$ have the necessary copper–oxygen plane, but the metal-oxide layer has been replaced with an alkaline earth chloride layer (*5, 6*). This yields an octahedral coordination about the copper with the oxide ions in the basal planes and two chloride ions in the apical positions. Recently, a perovskite-related phase has been discovered, $Ca_3Cu_2O_4Cl_2$, where the copper ions have a square pyramidal coordination with only one apical chloride (*7*). The transport properties of all of these oxychlorides have been reported and these materials are fairly insulating (*6*). For $Sr_2CuO_2Cl_2$ and $Ca_2CuO_2Cl_2$, the doping of charge carriers into the structure is difficult (*6*). Initial studies of $Ca_3Cu_2O_4Cl_2$ show that it is somewhat easier to substitute aliovalent ions into its structure (*8*), but other compounds should be found.

To approach this problem, we have synthesized a new class of copper oxychlorides which are related to the T* structure. The T* structure is known for compounds of the general formula, $La_{2-x-y}Ln_xSr_yCuO_4$ and $La_{2-x}Ln_xCuO_4$, and consists of two alternating metal-oxide layers—a rocksalt-like (La,Sr)–O layer (as found in the T structures) and a fluorite-like Ln–O layer (as found in the T′ structures) (*9–11*). In these new copper oxychlorides, the (La,Sr)–O layer has been replaced with a (Ca,Sr)–Cl layer. This yields a square pyramidal coordination about copper where the chloride ion occupies the lone apical position. The general formula of this new copper oxychloride is $MLnCuO_3Cl$, where M is Ca, Sr, or a combination of the two and Ln is a rare earth, Nd, Sm, Eu, or Gd. The structure of this compound along with that of the other two structures are shown in Fig. 1. A feature of this particular structure is that the layers between the copper–oxygen planes alternate between layers of Ln–O and M–Cl. With two different layers, one could substitute into the Ln–O layer to generate either an n-type (tetravalent cations) or a p-type (divalent cations) material while investigating the effect of the apical chloride on the properties of these compounds. In this paper, we report our preliminary findings on these new T* copper oxychlorides. In Section 2, we present the synthetic conditions required for the formation of $MLnCuO_3Cl$. In Section 3, we discuss the proposed structure of these compounds including an analysis of the relative sizes of the rare earth ions and the alkaline earth cations required for the stabilization of the T* structure. In Section 4, we report the basic physical properties of these compounds and discuss them in light of their parent compounds, $M_2CuO_2Cl_2$ and Ln_2CuO_4.

2. Synthetic Conditions

The $MLnCuO_3Cl$ copper oxychlorides were synthesized in the following manner. First stoichiometric amounts of CuO, Ln_2O_3, and SrO (CaO) are weighed with a 2-molar excess of $SrCl_2$ ($CaCl_2$) in a dry box. All of the reactants were at least reagent grade quality; the SrO was 99.5% pure and was purchased from ALFA. The excess alkaline earth chloride acts as a flux and is found to be necessary for the formation of the desired product. The starting materials are thoroughly ground and then pelletized. The resulting pellet is sintered in air at typically 820°C for 18 hr. The product is then separated from the flux through several washings with water. This synthetic technique is similar to that of Brixner who synthesized Sr_2VO_4Cl and $Sr_5(PO_4)Cl$ via excess $SrCl_2$ flux (*12*). The compounds are black, miceous, and stable to water (both $Sr_2CuO_2Cl_2$ and $Ca_2CuO_2Cl_2$ decompose

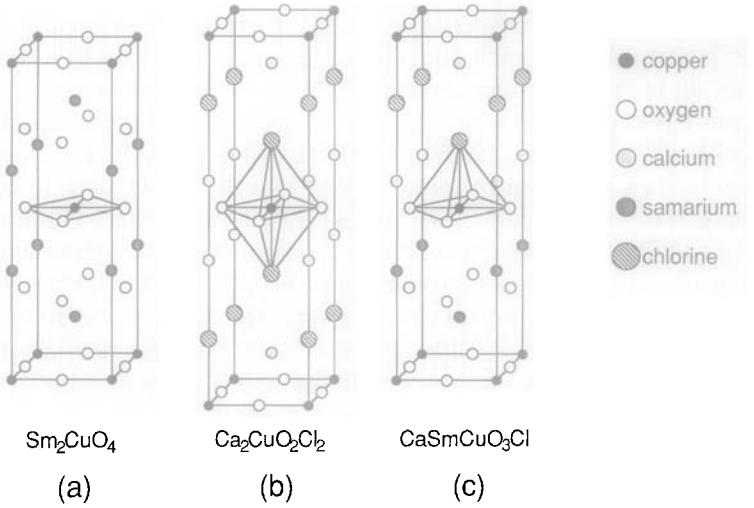

FIG. 1. The three tetragonal T phases: (a) T′ phase for Ln_2CuO_4 where Ln= Pr, Nd, Sm, Eu, Gd; (b) T phase for $M_2CuO_2Cl_2$ where M = Ca, Sr; and (c) T* phase for $MLnCuO_3Cl$.

readily when exposed to water). The lattice parameters and purity of the product were determined by powder X-ray diffraction (XRD). The relative amounts of Ca and Sr in the $Ca_{1-x}Sr_xLnCuO_3Cl$ compounds were determined using plasma emission spectroscopy (see Section 3.1).

Table I shows the rare earth and alkaline earth metal combinations that form the desired T* copper oxychlorides; the attempted syntheses of the T* oxychlorides with Ln = La, Pr, Tb, and Dy were unsuccessful. All of the mixed Ca–Sr compounds were formed with a 1 : 1 ratio of Ca to Sr in the initial mix. The synthetic conditions of three compounds, $SrNdCuO_3Cl$, $CaSmCuO_3Cl$, and $CaGdCuO_3Cl$ were investigated in detail to obtain single phase materials. For $SrNdCuO_3Cl$, it was found that it formed in air when the temperature was in the range of 760°C (reaction time of several days) to 890°C (10 hr). At 890°C, the $SrNdCuO_3Cl$ phase in $SrCl_2$ flux decomposes into $Sr_2CuO_2Cl_2$ and Nd_2CuO_4 with longer reaction times; how-

TABLE I

LATTICE PARAMETERS FOR $MLnCuO_3Cl$[a]

Compound	a (Å) exp	c (Å) exp	a (Å) calc	c (Å) calc
$SrNdCuO_3Cl$	3.956(1)	13.880(2)	3.956	13.887
$Ca_{0.72}Sr_{0.28}NdCuO_3Cl$	3.926(1)	13.665(1)	3.921	13.620
$Ca_{0.78}Sr_{0.22}SmCuO_3Cl$	3.910(1)	13.559(1)	3.916	13.637
$CaSmCuO_3Cl$	3.901(1)	13.430(1)	3.886	13.457
$Ca_{0.80}Sr_{0.20}EuCuO_3Cl$	3.898(1)	13.519(2)	3.891	13.450
$CaEuCuO_3Cl$	3.892(1)	13.405(1)	3.881	13.431
$Ca_{0.79}Sr_{0.21}GdCuO_3Cl$	3.893(1)	13.517(2)	3.889	13.486
$CaGdCuO_3Cl$	3.888(1)	13.389(1)	3.878	13.418

[a] All mixed Ca–Sr compounds were reacted with a 50% Ca : 50% Sr flux.

ever, regardless of the reaction time or temperature, there was always a small amount of $Sr_2CuO_2Cl_2$ and Nd_2CuO_4 present. The use of an oxygen atmosphere in this system was found to reduce the amount of $Sr_2CuO_2Cl_2$ and Nd_2CuO_4 relative to that of the product; however, these two impurities were always found. We also varied the amount of SrO to Nd_2O_3 to determine whether Sr could replace Nd and vice versa. The XRD lines due to $SrNdCuO_3Cl$ did not shift with different SrO/Nd_2O_3 ratios, which implies that this compound is a line phase with a Sr : Nd ratio of one.

The effect of the flux was also investigated for the $SrNdCuO_3Cl$ system. Without any excess $SrCl_2$, no $SrNdCuO_3Cl$ was formed. The amount of product increased as the amount of flux increased with a maximum at 200% mole excess of $SrCl_2$. The replacement of some of the $SrCl_2$ flux with $CaCl_2$ was found to suppress the formation of Nd_2CuO_4 and subsequently enhance the formation of $Ca_{1-x}Sr_xNdCuO_3Cl$. The compounds substituted with calcium appeared to be single phase with extra lines in XRD only from the flux; after washing, no extra lines were seen.

To prepare single phase $CaSmCuO_3Cl$, the reaction conditions had to be modified slightly. The reaction temperature was increased to 840°C and intermediate regrindings were needed. The sample was heated for 6 hr, reground, and then heated for three more 18-hr periods with regrindings. After the initial 6-hr reaction period, a new peak (in addition to peaks from $CaSmCuO_3Cl$ and $Ca_2CuO_2Cl_2$) was observed in XRD at $d \approx$ 20.8Å. We believe that the 20.8-Å peak is due to an intermediate phase with two layers of Ca–Cl (instead of one) alternating with one layer of Sm–O as the stacking sequence between the copper–oxygen planes. This will be discussed further in the structural properties of these compounds.

$CaGdCuO_3Cl$ required significantly different synthetic conditions to obtain the desired composition. The reaction temperature was increased to 920°C and the flux was reduced so that only a half-mole excess of $CaCl_2$ was present. These conditions yielded relatively X-ray pure prodcut (a few impurity lines were observed at <5% relative intensity). When the reaction was initially carried out at 820°C with 200% mole excess of $CaCl_2$, no $CaGdCuO_3Cl$ was formed; an unknown hygroscopic phase had formed instead.

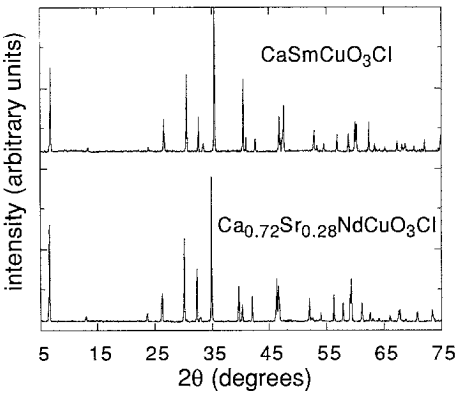

FIG. 2. Powder X-ray diffraction spectra for $CaSmCuO_3Cl$ and $Ca_{0.72}Sr_{0.28}NdCuO_3Cl$ at 300 K. Monochromatized Cu$K\alpha$ radiation was used.

Finally, the growth of single crystals was attempted for $CaSmCuO_3Cl$. The ideal conditions for crystal growth were found to be with an oxygen atmosphere at 860°C for several days (yielding crystals up to 0.2 mm × 0.2 mm × 0.04 mm). In an oxygen atmosphere, the reaction temperature had to be increased to form $CaSmCuO_3Cl$; below 860°C, the reaction did not occur. At the lower temperatures, an impurity phase analogous to that seen in $CaGdCuO_3Cl$ reactions with 2-molar excess flux was observed.

3. Structural Studies

3.1 Basic Characterization

The powder patterns of washed $CaSmCuO_3Cl$ and $Ca_{0.72}Sr_{0.28}NdCuO_3Cl$ are shown in

TABLE II

POWDER DIFFRACTION DATA OF T* OXYCHLORIDES (*P4/nmm* Symmetry)

	$CaSmCuO_3Cl$ a = 3.901(1) Å c = 13.430(1) Å				$Ca_{0.72}Sr_{0.28}NdCuO_3Cl$ a= 3.926(1) Å c = 13.665(1) Å			
$h\ k\ l$	d_{obs}(Å)	d_{calc}(Å)	I_{obs}	I_{calc}	$h\ k\ l$	d_{obs}(Å)	d_{calc}(Å)	I_{obs}
0 0 1	13.40	13.43	58	—	0 0 1	13.64	13.66	50
0 0 2	6.71	6.72	3	4	0 0 2	6.83	6.83	3
0 0 3	4.477	4.477	1	1	0 0 3	—	4.555	
1 0 1	3.750	3.746	4	22	1 0 1	3.773	3.773	10
1 0 2	3.372	3.373	22	48	0 0 4	3.416	3.414	10
0 0 4	3.359	3.357	6	1	1 0 2	3.400	3.404	28
1 0 3	2.941	2.941	54	71	1 0 3	2.974	2.974	86
1 1 0	2.759	2.758	25	53	1 1 0	2.777	2.776	73
1 1 1	2.701	2.702	3	4	0 0 5	2.733	2.733	1
0 0 5	2.686	2.686	6	1	1 1 1	2.719	2.720	5
1 0 4	2.544	2.545	100	100	1 0 4	2.578	2.577	100
0 0 6	2.238	2.238	50	7	0 0 6	2.278	2.277	22
1 0 5	2.2112	2.2112	10	6	1 0 5	2.2432	2.2429	13
1 1 4	2.1311	2.1313	9	24	1 1 4	2.1544	2.1543	24
2 0 0	1.9501	1.9505	25	48	1 0 6	1.9693	1.9699	14
1 0 6	1.9414	1.9414	9	2	2 0 0	1.9630	1.9629	59
2 0 1	1.9304	1.9302	5	12	0 0 7	1.9520	1.9521	42
1 1 5	1.9234	1.9243	12	18	1 1 5	1.9474	1.9475	22
0 0 7	1.9183	1.9185	32	5	2 0 1	1.9435	1.9429	13
1 1 6	1.7387	1.7380	14	18	1 1 6	1.7605	1.7607	15
1 0 7	1.7220	1.7216	5	1	1 0 7	—	1.7479	
2 1 2	1.6881	1.6885	6	13	0 0 8	—	1.7081	
0 0 8	1.6789	1.6787	2	1	2 1 2	1.6993	1.7004	11
2 1 3	1.6260	1.6255	11	25	2 1 3	1.6371	1.6382	27
1 1 7	1.5750	1.5750	12	10	1 1 7	1.5965	1.5968	12
2 1 4	—	1.5480	—	38	1 0 8	1.5658	1.5662	27
1 0 8	1.5425	1.5420	21	11	2 1 4	1.5613	1.5615	44
0 0 9	1.4926	1.4922	19	3	0 0 9	1.5183	1.5183	14
2 0 6	1.4706	1.4705	21	7	2 0 6	1.4866	1.4868	13
2 1 5	—	1.4630	—	2	2 1 5	1.4764	1.4771	7
1 1 8	1.4343	1.4340	3	3	1 1 8	—	1.4547	
1 0 9	1.3938	1.3937	7	4	1 0 9	1.4161	1.4161	5
2 2 0	1.3789	1.3792	5	14	2 2 0	1.3880	1.3880	17
2 0 7	1.3672	1.3678	5	6	2 0 7	1.3844	1.3841	11
0 0 1 0	1.3433	1.3430	4	1	0 0 1 0	1.3669	1.3665	4
1 1 9	1.3127	1.3125	8	2	1 1 9	1.3323	1.3321	7
1 0 1 0	1.2701	1.2698	11	5	1 0 1 0	1.2914	1.2905	8

Fig. 2. These data were collected at room temperature with a Scintag PAD V X-ray diffractometer and monochromatized Cu$K\alpha$ radiation; they can be fit to a tetragonal cell of *P4/nmm* symmetry with a= 3.901(1) Å and c = 13.430(1) Å for $CaSmCuO_3Cl$ and with a= 3.926(1) Å and c = 13.665(1) Å for $Ca_{0.72}Sr_{0.28}NdCuO_3Cl$. The assignment of Miller indices and the observed intensities for the reflections are shown in Table II. Of the 22 possible reflections of this cell below $2\theta = 50°$, 19 have been observed in the XRD

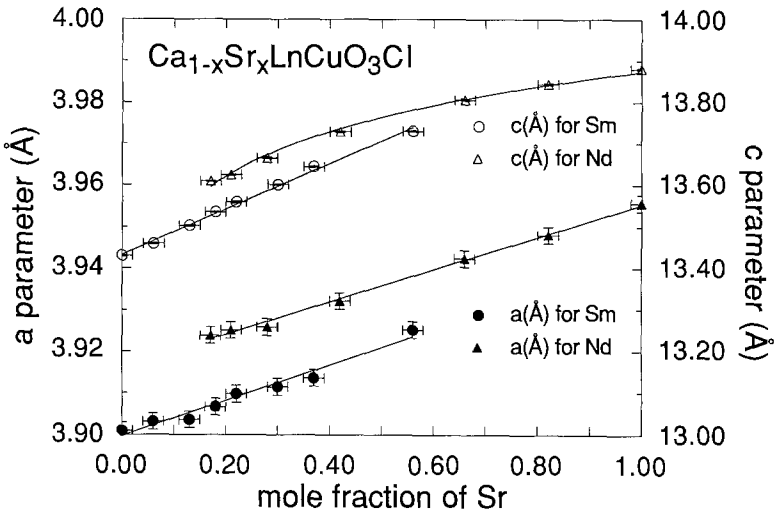

FIG. 3. The lattice parameters for $Ca_{1-x}Sr_xLnCuO_3Cl$ (Ln = Nd, Sm) as determined by X-ray powder diffraction. The mole fraction of Sr was determined by plasma emission. The endpoints at x= 0.17 for $Ca_{1-x}Sr_xNdCuO_3Cl$ and x = 0.56 for $Ca_{1-x}Sr_xSmCuO_3Cl$ can be related to the size requirements of the T* copper oxychlorides.

for $CaSmCuO_3Cl$. In these compounds, only one systematic absence is observed: the $h+k = 2n + 1$ reflections for [hk0] which are characteristic of either $P4/n$ or $P4/nmm$ symmetry. Because $P4/nmm$ symmetry has been observed previously in the T* copper oxides, our observation of this systematic absence suggests the structure in Fig. 1c with $P4/nmm$ symmetry. This conclusion is further supported by a calculation of the X-ray powder pattern intensities for $CaSmCuO_3Cl$. With bond distances assumed to be equal to those found in $Ca_2CuO_2Cl_2$ and Sm_2CuO_4, the XRD intensities for the proposed T* structure were calculated; the results are shown in Table II. The calculated and the observed intensities are in fairly good agreement considering that this calculation had no adjustable parameters.

The proposed T* structure in Fig. 1c is also supported by a calculation of the lattice constants based on this structure. A simple estimate can be made by averaging the lattice parameters of the two parent compounds, $Ca_{2-x}Sr_xCuO_2Cl_2$ and Ln_2CuO_4. The calculated values are shown in Table I. Both the a and the c parameters are predicted within 5% of their experimental values; therefore, we conclude that the structure depicted in Fig. 1c is correct and the coordination of copper is square pyramidal with an apical chloride ion. Such a geometry for copper is quite common in oxides where the apical positions are filled with oxide ions; and in fact, Sowa *et al.* have synthesized $Ca_3Cu_2O_4Cl_2$, a modified Ruddlesden-Popper phase of $Ca_2CuO_2Cl_2$, which has the identical coordination of copper as proposed here for $MLnCuO_3Cl$ copper oxychlorides (*7*).

The electron microprobe analysis was performed with a JEOL 8600 Superprobe to confirm the stoichiometry of $CaSmCuO_3Cl$. Eight independent measurements indicated a formula of $Ca_{1.00}Sm_{1.02}Cu_{0.97}Cl_{1.01}O_x$ with a ± 0.05 error for each ion. Some of the less regular crystals showed inclusions of another material in them with a needle-like morphology (the $CaSmCuO_3Cl$ crystals are square plates). These inclusions were only

TABLE III

STRUCTURAL FACTORS FOR T* COPPER OXYCHLORIDES AND OXIDES

Compound	$r_{T'}$ (Å)[a]	r_T (Å)[b]	$r_{T'}/r_T$
$SrNdCuO_3Cl$	1.249	1.450	1.16
$Ca_{0.72}Sr_{0.28}NdCuO_3Cl$	1.249	1.356	1.09
$Ca_{0.83}Sr_{0.17}NdCuO_3Cl$	1.249	1.342	1.07
$Ca_{0.44}Sr_{0.56}SmCuO_3Cl$	1.219	1.393	1.14
$Ca_{0.78}Sr_{0.22}SmCuO_3Cl$	1.219	1.349	1.11
$CaSmCuO_3Cl$	1.219	1.320	1.08
$Ca_{0.80}Sr_{0.20}EuCuO_3Cl$	1.206	1.350	1.12
$CaEuCuO_3Cl$	1.206	1.320	1.09
$Ca_{0.79}Sr_{0.21}GdCuO_3Cl$	1.193	1.354	1.13
$CaGdCuO_3Cl$	1.193	1.320	1.11
$La_{0.9}Y_{0.8}Sr_{0.3}CuO_4$	1.187	1.384	1.17
$LaDy_{0.8}Sr_{0.2}CuO_4$	1.194	1.375	1.15
$La_{0.9}Gd_{0.9}Sr_{0.2}CuO_4$	1.204	1.375	1.14
$La_{1.2}Dy_{0.8}CuO_4$	1.194	1.356	1.14
$Nd_{1.32}Sr_{0.41}Ce_{0.27}CuO_4$	1.207	1.362	1.13
$La_{1.1}Eu_{0.8}Sr_{0.1}CuO_4$	1.225	1.365	1.11
$La_{1.4}Tb_{0.6}CuO_4$	1.228	1.356	1.10
$LaNdCuO_4$	1.249	1.356	1.09

[a] For 8-coordinate site.
[b] For 9-coordinate site.

a few percent of the total material and were found to have a composition of approximately Sm_3CuClO_5, apparently a new phase.

Direct-current plasma-emission spectroscopy was performed to determine the amounts of Ca and Sr in the substituted $Ca_{1-x}Sr_xLnCuO_3Cl$ compounds since the washing away of excess flux leaves these values in question. A Beckman-Spectrametrics basic multiatomic emission spectrometer with a Spectrajet III DC plasma source was used for the measurements. The Sr and especially the Ca lines were found to be quite sensitive to the presence of rare earths in the matrix; therefore, all standard solutions were made with a similar composition to the compound being studied. For the $Ca_{1-x}Sr_xLnCuO_3Cl$ compounds, only Ca, Sr, and *Ln* ions were probed; therefore, the Ca/Sr ratio is overdetermined threefold. The resulting data are presented in Tables I and III and are incorporated into Fig. 3.

The plasma emission technique was also used as a further check of the stoichiometry and the purity of the $CaSmCuO_3Cl$ and $Ca_{0.72}Sr_{0.28}NdCuO_3Cl$ samples (Cu was also measured in these samples). For $CaSmCuO_3Cl$, the weight percentage of each cation was found to be 12.9 ± 0.7% Ca, 47.2 ± 1.7% Sm, and 18.6 ± 0.3% Cu. If one compares these results to the weight percentages predicted for an ideal $CaSmCuO_3Cl$ stoichiometry, the mole fraction of each cation is 0.99 ± 0.06 Ca, 1.06 ± 0.04 Sm, and 0.99 ± 0.02 Cu. For $Ca_{0.72}Sr_{0.28}NdCuO_3Cl$, the weight percentages were found to be 7.8 ± 0.2% Ca, 7.2 ± 0.1% Sr, 40.8 ± 0.2% Nd, and 18.45 ± 0.02% Cu which corresponds to 0.67 ± 0.02 Ca, 0.28 ± 0.01 Sr, 0.98 ± 0.01 Nd, and 1.00 ± 0.02 Cu. The errors correspond to the scatter in the measure-

ments and do not reflect any systematic errors such as matrix sensitivity. Ca is especially prone to matrix sensitivity; therefore, we have relied on the Sr result in the stoichiometry of $Ca_{0.72}Sr_{0.28}NdCuO_3Cl$. Nonetheless, these results support the stoichiometry and purity of these two samples.

Single crystal X-ray diffraction analysis was attempted on $CaSmCuO_3Cl$ with a CAD4 X-ray diffractometer with Mo$K\alpha$ radiation. A set of 580 independent reflections were collected with a cell that matched the lattice parameters found in the powder XRD (a = 3.896(1) Å, b = 3.901(1) Å, c = 13.422(1) Å, α = 89.96(1)°, β = 90.04(1)° and γ = 90.01(1)° for the single crystal cell); however, the Patterson map of the data had an abnormally short vector (<1 Å) with relatively strong intensity, which indicated that the crystal was twinned. All the crystals appeared to be twinned in some manner; we are presently attempting to grow better quality crystals to solve the structure.

The twinning mechanism is likely to be due to stacking faults, because of the nature of these T* compounds. The faults would be an error in the alternating sequence of Ca–Cl and Sm–O layers between the copper–oxygen sheets. This hypothesis is supported by the observation of the interemediate in XRD with $d \approx 20.8$ Å. This intermediate is likely a compound with two Ca–Cl layers alternating with one Sm–O layer. The estimated c parameter for this compound would be 20.94 Å (14.98 Å from c of $Ca_2CuO_2Cl_2$ and 5.97 Å from $c/2$ of Sm_2CuO_4). An observation of this intermediate is consistent with the proposed structure, and it appears that annealing is necessary to provide the long range order of the T* structure.

3.2 $Ca_{1-x}Sr_xSmCuO_3Cl$ and $Ca_{1-x}Sr_xNdCuO_3Cl$

When the rare earth is neodymium, the pure Ca phase ($CaNdCuO_3Cl$) does not exist; and when the rare earth is samarium, the pure Sr phase ($SrSmCuO_3Cl$) does not exist. The effective ionic radius of Nd^{3+}, in an 8-coordinate site, is 1.249 Å, and the ionic radius of Sm^{3+} is only 0.03 Å smaller at 1.219 Å (*13*); thus, the stability of the T* oxychlorides is very sensitive to the size of rare earth. This sensitivity is not unexpected; the T* copper oxides have been shown to be very sensitive to the cation size and show ordering of the cations on the basis of size (*10, 11*). We have investigated the substitutions of $Ca_{1-x}Sr_xLnCuO_3Cl$ with Ln = Nd, Sm to elucidate on the size requirements of T* phase formation. The lattice parameters of these substitutions are shown in Fig. 3. The a and c parameters of either Ln = Sm or Nd increase linearly as the amount of Sr increases, showing that the larger cation, strontium, simply increases the overall volume of the cell. There is a slight curvature in the c parameter plot (but not the a parameter) for $Ca_{1-x}Sr_xNdCuO_3Cl$; this reflects that the smaller Ca occupies a position which is relatively unstrained in the c direction and that Sr substitution does not expand that direction as much. The linearity in the a parameter data suggests that the copper–oxygen sheet is relatively unstrained and that it freely adjusts to accommodate the electronic and structural requirements of the particular T* phase. All of the a parameter distances reported here are well within typical copper–oxygen bond distances found in Ln_2CuO_4 with the T′ structure (*10*).

The data in Fig. 3 show two phases which are the limits of stability for the T* phase. $Ca_{0.83}Sr_{0.17}NdCuO_3Cl$ represents the smallest difference between the effective ionic radius of the rare earth (1.249 Å) and the alkaline earth metal (1.374 Å), whereas, $Ca_{0.44}Sr_{0.56}SmCuO_3Cl$ represents one of the largest differences (1.219 Å and 1.439 Å, respectively). Therefore, the data in Fig. 3 contain the size requirements for T* copper oxychlorides studied here. To quantify these requirements, we use the ratio of the

radius of the alkaline earth metal (the T cation) to the radius of the rare earth (the T′ cation). Bringley *et al.* have used this ratio in their study of T* copper oxides (*14*). This ratio simply quantifies the preference of the larger cations for the nine-coordinate T site and the smaller cations for the 8-coordinate T′ site. The calculated values of $r_T/r_{T'}$ for the T* oxychlorides are shown in Table III along with $r_T/r_{T'}$ for the T* oxides. We have used the 8- and 9-coordinate crystalline radius (CR) ionic radii from Shannon's tables (*13*). Coincidentally, the values are roughly the same for the two classes of T* compounds; the values are $1.07 \leq r_T/r_{T'} \leq 1.16$ for the T* oxychlorides and $1.08 \leq r_T/r_{T'} \leq 1.18$ for the T* oxides. The agreement between these two classes of compounds is fortuitous and simply reflects that the *Ln* cation (in both compounds) is always a middle rare earth and the *M* cation is an alkaline earth metal (in the oxychlorides) or a La^{3+} ion (in the oxides); La^{3+} has a similar ionic radius as Ca^{2+}.

4. Physical Properties

4.1 Resistivity of Annealed Samples

High temperature ac impedance measurements were performed on polycrystalline samples of $CaSmCuO_3Cl$ and $Ca_{0.72}Sr_{0.28}NdCuO_3Cl$ in oxidizing and reducing atmospheres. A Solartron Model 1250 frequency analyzer and a Model 1186 electrochemical interface were used to collect the data via a Hewlett–Packard 9816 computer; a frequency range from 10 to 65 kHz was used (*15*). Contacts were made with platinum paste on disk-shaped samples which were 1- to 2-mm thick. Each sample was annealed in the appropriate atmosphere at 650°C for 3 hr. The resistivity data from 100 to 600°C for the argon-annealed samples of $CaSmCuO_3Cl$ and $Ca_{0.72}Sr_{0.28}NdCuO_3Cl$ are shown in Fig. 4 and show activation energies of 0.54 and 0.47 eV, respectively. At temperatures below 200°C, these samples show a semicircular frequency response characteristic of ionic conduction. Figure 5 shows a typical frequency response for $CaSmCuO_3Cl$. From several low temperature semicircles, we have estimated the relaxation time, τ, by noting the frequency at the maximum of the semicircle. A $\tau_0 \approx 2 \times 10^{-12}$ sec is then calculated for $\tau = \tau_0 \exp(E_a/kT)$ relationship. These relaxation times and activation energies are typical of either oxide ion or oxide vacancy diffusion (*15*). Because these samples were annealed in an inert atmosphere, we assign the ionic conductivity in the samples to be the motion of oxygen vacancies. Thermogravimetric measurements (TGA) were performed on these annealed samples to determine the amount of oxygen entering/leaving the samples. The weight loss/gain was less than 0.2% (the sensitivity of our instrument) indicating that the amount of oxygen leaving these samples is small. The assignment of oxygen vacancy motion is supported by the ease of vacancy formation in $Nd_{1.85}Ce_{0.15}CuO_{4-x}$ (*16, 17*). In the resistivity measurements by Ganguly and Rao, Sm_2CuO_4 and Nd_2CuO_4 above 600°C showed an activation energy of ~0.70 eV (*18*). We believe this conductivity is due to vacancy motion in their samples, although an electronic conductivity component cannot be ruled out (*19*).

The resistivity data for the oxygen-annealed samples of $CaSmCuO_3Cl$ and $Ca_{0.72}Sr_{0.28}NdCuO_3Cl$ are also shown in Fig. 4. The $CaSmCuO_3Cl$ sample indicated electrical conductivity with semiconducting behavior—a resistivity of ~100 Ω · cm at 300 K and an activation energy of 0.12 eV. Miller *et al.* found for the related oxychloride, $Sr_2CuO_2Cl_2$, that the resistivity is >3000 Ω · cm at 300 K with an activation energy of ~0.5 eV (*6*), while Ganguly and Rao have found that Sm_2CuO_4 and Nd_2CuO_4 have resistivities of ~100 Ω · cm at 300 K and an activation energy of 0.15 eV at temperatures below 600 K (*18*). Clearly, the magnitude of the resistivity and activation energy of

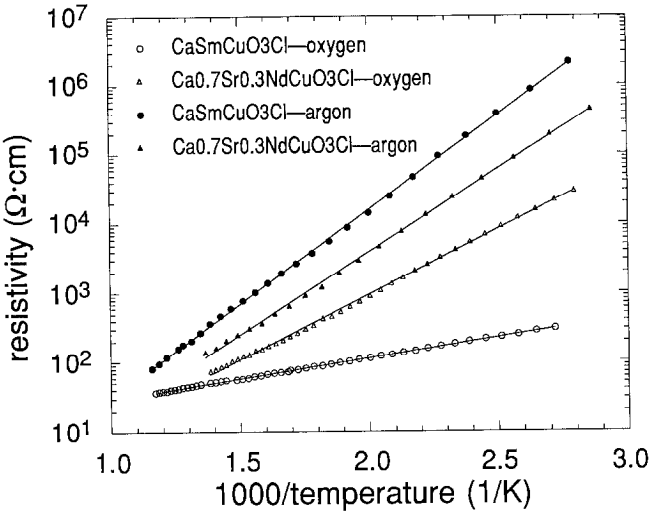

FIG. 4. The resistivity of $CaSmCuO_3Cl$ and $Ca_{0.72}Sr_{0.28}NdCuO_3Cl$ from 100 to 600°C. The oxygen-annealed $CaSmCuO_3Cl$ sample showed electrical conductivity with an activation barrier of 0.12 eV. The two argon-annealed samples and the oxygen-annealed $Ca_{0.72}Sr_{0.28}NdCuO_3Cl$ sample all showed ionic conductivity.

$CaSmCuO_3Cl$ most closely resembles that of the undoped T′ copper oxide and the apical chloride appears to have a negligible effect on the resistivity in this compound.

The ac impedance measurements for $Ca_{0.72}Sr_{0.28}NdCuO_3Cl$ in an oxygen atmosphere indicated an activation energy of 0.37 eV. The conductivity has been reduced by roughly an order of magnitude, indicating that there may be a small electrical component to it; however, clear semicircles were observed at the lower temperatures, indicating that the conductivity is mostly ionic. In light of the semiconducting behavior of the oxygen-annealed $CaSmCuO_3Cl$ sample, the observation of primarily ionic conductivity for $Ca_{0.72}Sr_{0.28}NdCuO_3Cl$ was puzzling, so we investigated two other samples. One was a sample of $Ca_{0.72}Sr_{0.28}NdCuO_3Cl$ that was prepared with a synthetic procedure identical to that used for $CaSmCuO_3Cl$ (synthesis at 840°C with several regrindings) to see whether electrical conductivity could be observed in $Ca_{0.72}Sr_{0.28}NdCuO_3Cl$. This treatment yielded no difference in the resistivity of oxygen- or argon-annealed $Ca_{0.72}Sr_{0.28}NdCuO_3Cl$, indicating that the resistivity measurements are intrinsic and not a manifestation of the synthetic procedure. Second, we checked the resistivity of $Ca_{0.44}Sr_{0.56}SmCuO_3Cl$, which has approximately the same a

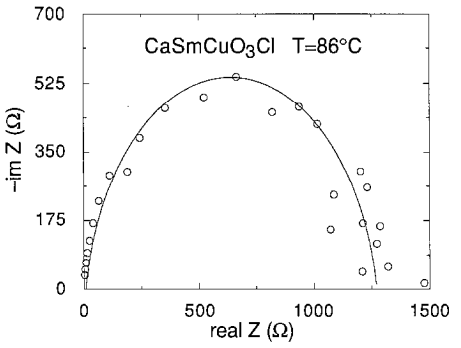

FIG. 5. Typical AC impedance response for an ionic conducting sample. The signal is attributed to the motion of oxygen vacancies. The solid line is a semicircular fit to provide a guide to the eye.

parameter as $Ca_{0.72}Sr_{0.28}NdCuO_3Cl$, to determine whether the longer copper–oxygen bond distance in $Ca_{0.72}Sr_{0.28}NdCuO_3Cl$ may be a factor. The $Ca_{0.44}Sr_{0.56}SmCuO_3Cl$ sample showed electrical conductivity and had similar characteristics to those of the CaSm CuO_3Cl sample.

A possible mechanism for the formation of oxygen vacancies in $MLnCuO_3Cl$ is that the large excess of flux used during synthesis results in some Ca^{2+} ions being doped into the *Ln*–O layer either as a Ca–Cl pair or as a Ca^{2+} ion with an oxygen vacancy. Either possibility would result in charge compensation, therefore no charge carriers should be introduced into the copper–oxygen sheet. Subsequent annealing of the samples in argon then causes chlorine to leave irreversibly from the Ca–Cl defects leaving an oxygen vacancy and/or resulting in even more oxygen vacancies from possible Ca^{2+} defects in the *Ln*–O layer. When the sample is annealed in an O_2 atmosphere, the vacancies are replaced with oxygen. We have found some evidence that chlorine does leave the structure. Samples of CaSmCu O_3Cl and $Ca_{0.72}Sr_{0.28}NdCuO_3Cl$ that were not annealed (i.e., samples that are charge compensated and have no charge carriers) had several orders of magnitude higher resistance than any of the annealed samples. Also, TGA measurements of unannealed samples showed a ~1% irreversible weight loss from 100 to 600°C (we took care to make sure these samples were dry; and if water was present, it should have been gone by 200°C). Regardless of subsequent heat treatments, annealed samples could not be returned to their original highly resistive state or their original weight (that is, annealing introduced charge carriers). Thus in CaSm CuO_3Cl, the amount of Ca^{2+} defects is high enough to introduce a significant amount of holes into the copper–oxygen sheet (when the sample is annealed in oxygen), whereas in $Ca_{0.72}Sr_{0.28}NdCuO_3Cl$, the amount of defects is too low. Room temperature Seebeck measurements on oxygen-annealed CaSm CuO_3Cl indicate *p*-type carriers consistent with this hypothesis.

4.2 Magnetic Properties

Because of the presence of a rare earth ion in $MLnCuO_3Cl$, the magnetic properties are expected to be dominated by the spin of this ion. Magnetic measurements on $Sr_2Cu O_2Cl_2$ indicate that copper spins in this compound order antiferromagnetically at a Néel temperature of 250 K with a residual moment of 0.34 μ_B (*20*). Other copper oxides, both with the T and the T′ structure have Néel temperatures in this range and a small copper moment (*21, 22*), therefore we expect that these T* oxychlorides act similarly. For our analysis, we shall ignore the copper moment and focus on the role of the rare earth.

The temperature dependence of the reciprocal magnetic susceptibility of polycrystalline $Ca_{0.72}Sr_{0.28}NdCuO_3Cl$ is shown in Fig. 6. To fit the data, one must take into account the splitting of the $^4I_{9/2}$ ground state of Nd^{3+}. The Nd^{3+} ion is in the presence of a tetragonal crystal field which is approximated by a cubic field. The presence of a cubic field results in a Kramer's doublet ground state and two fourfold degenerate excited states. This approximation was used to fit the magnetic data of Nd_2CuO_4 by Saez Puche *et al.* (*23*). Seaman *et al.* have improved the fit of Nd_2CuO_4 by adding a mean field term to account for interaction between Nd^{3+} spins (*24*). Because Nd_2CuO_4 is the parent compound of $Ca_{0.72}Sr_{0.28}NdCuO_3Cl$, we adopted their approach to fit our data. The equation for the susceptibility is given by

$$\frac{1}{\chi} = \frac{1}{\chi(Nd^{3+})} - \frac{\Theta}{C}, \qquad (1)$$

where C is the Curie constant, Θ is the Curie–Weiss temperature and $\chi(Nd^{3+})$ is

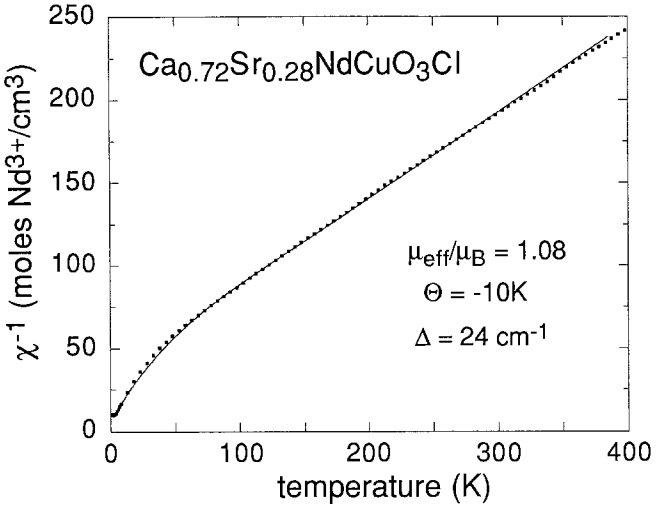

FIG. 6. The reciprocal magnetic susceptibility of polycrystalline $Ca_{0.72}Sr_{0.28}NdCuO_3Cl$ from 2 to 400 K. The solid line corresponds to a fit of Eq. (1).

$$1/\chi(Nd^{3+}) = \frac{\mu_{eff}^2 N_A}{\Delta} \times \{[(0.1483x_1 + 0.2396x_2 - 0.3879x_3) + \frac{\Delta}{kT}(6.064x_1 + 4.031x_2 + 1.680x_3)] \div (2x_1 + 2x_3 + x_3)\} \quad (2)$$

$$x_1 = \exp(19.59\Delta/kT),$$
$$x_2 = \exp(-9.11\Delta/kT),$$
$$x_3 = \exp(-20.95\Delta/kT).$$

where μ_{eff} is the effective magnetic moment and Δ is the crystal field parameter. Theoretically, μ_{eff} for Nd^{3+} should equal $\sqrt{2}g\mu_B$ with the Landé factor, g equal to 8/11; this corresponds to a theoretical value for μ_{eff}/μ_B of 1.03. Because of possible interactions with the copper ions (*25*), we have kept μ_{eff} as an adjustable parameter. The fit in Fig. 6 indicates $\mu_{eff}/\mu_B = 1.08 \pm 0.01$, which is reasonably close to the theoretical value. Also, $\Theta = -10 \pm 1$ K implies that there are antiferromagnetic interactions between the spins; however, they appear to be reduced as compared to Nd_2CuO_4, where $\Theta = -23$ K. The $\Delta = 24 \pm 1$ cm^{-1} from our fit suggests that the excited crystal field states are located 285 cm^{-1} (410 K) and 970 cm^{-1} (1390 K) above the ground state. These values are comparable to the excited state energies in Nd_2CuO_4 at 337 cm^{-1} (485 K) and 1155 cm^{-1} (1660 K) (*23*).

The reciprocal magnetic susceptibility of polycrystalline $CaSmCuO_3Cl$ is shown in Fig. 7. Because of the $^6H_{7/2}$ excited state is rather close to the $^6H_{5/2}$ ground state, the applied magnetic field mixes an appreciable fraction of the excited state into the ground state; this gives rise to a temperature-independent Van Vleck susceptibility contribution. Seaman has fit the susceptibility of Sm_2CuO_4 by the following formula, which we have used to fit our data of $CaSmCuO_3Cl$,

$$\chi = N_A\left(\frac{\mu_{eff}^2}{3k(T-\Theta)} + \frac{20\,\mu_B^2}{7k\Delta E}\right), \quad (3)$$

where ΔE is the average energy of the $^6H_{7/2}$ multiplet (*24*). Our fit of the magnetic susceptibility of $CaSmCuO_3Cl$ yields $\Delta E = 550 \pm 10$ cm^{-1} (790 K), $\Theta = -5.3 \pm 0.5$ K, and $\mu_{eff}/\mu_B = 0.38 \pm 0.02$. The fit is best at the

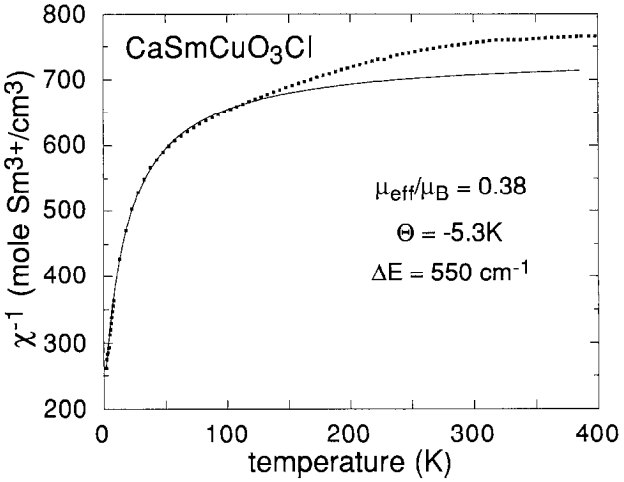

FIG. 7. The reciprocal magnetic susceptibility of polycrystalline $CaSmCuO_3Cl$ from 2 to 400 K. The solid line corresponds to a fit of Eq. (3). No ordering of the Sm^{3+} spins is observed to 2 K, unlike Sm_2CuO_4, where the Sm^{3+} spins order at 5.8 K.

lower temperatures where Eq. (3) is the most accurate. These values are similar to the values of Sm_2CuO_4 reported by Seaman of $\Delta E = 730$ cm^{-1} (1050 K), $\Theta = -8.3$ K, and $\mu_{eff}/\mu_B = 0.33$. The greatest difference is with ΔE; our value of 550 cm^{-1} is significantly smaller than that of the free ion at ~1000 cm^{-1}. The above treatment assumes an average energy for the $^6H_{7/2}$ excited state and neglects any crystal field effects. It is likely that our low ΔE is from a fit that emphasizes the lowest crystal field component of the $^6H_{7/2}$ state.

Several conclusions can be drawn from the magnetic-susceptibility data. For both $CaSmCuO_3Cl$ and $Ca_{0.72}Sr_{0.28}NdCuO_3Cl$, the Curie–Weiss temperature is closer to zero than in the corresponding copper oxide, implying a reduction in the antiferromagnetic correlations between the rare earths. Also down to 1.8 K, we have not observed any ordering of the rare earth spins in $CaSmCuO_3Cl$ and $Ca_{0.72}Sr_{0.28}NdCuO_3Cl$, whereas in Sm_2CuO_4 and Nd_2CuO_4, the rare earths order at 5.95 and 1.7 K, respectively. The reductions of antiferromagnetic interactions are likely caused by the physical separation of the *Ln*–O layers. However, the magnetic susceptibilities of $CaSmCuO_3Cl$ and $Ca_{0.72}Sr_{0.28}NdCuO_3Cl$ are quite similar to the susceptibilities of Sm_2CuO_4 and Nd_2CuO_4 above the rare earth Néel temperature (as manifested by similar values of μ_{eff}/μ_B, Δ, and ΔE). Thus, the local environment of the rare earth is approximately the same in T* copper oxychlorides as in their parent T′ copper oxide.

5. Conclusions

The chemistry of these new T* copper oxychlorides is interesting and several criteria must be met for these compounds to form. Because the T* structure consists of alternating types of layers between the copper–oxygen sheets, the cations must be separated; this is accomplished by difference in charge and size. The size requirement is reflected by a stability range of $1.07 \leq r_T/r_T' \leq 1.16$ for these T* copper oxychlorides. In the T* copper oxides, the size requirement is the only factor in separating the two layers

which make those compounds difficult to synthesize in pure form because the T phase, the T′ phase, and the T* phase are only minor modifications of the same basic structure. In the T* copper oxychlorides, the synthetic conditions are more lenient because of the great difference between those of $M_2CuO_2Cl_2$ and Ln_2CuO_4. $MLnCuO_3Cl$ begins to form at ~800°C—where Ln_2CuO_4 just begins to form, but well above the temperature where $M_2CuO_2Cl_2$ forms (*6*).

The MCl_2 flux is essential in the formation of T* oxychlorides. It provides a chlorine-rich environment while maintaining the oxidizing conditions necessary for the divalent copper ion. The exact amount of flux is critical: when no flux is present, the oxygen-rich T′ copper oxide forms; and when a large excess of flux is present (as in the $CaGdCuO_3Cl$ reaction), a new chlorine-rich phase is formed instead of the T* copper oxychloride. This indicates a delicate balance between the activities of oxygen and chlorine is needed to form the T* phase. Perhaps controlled atmospheres with fixed ratios of chlorine gas to oxygen gas may be a better way to synthesize these compounds. This sensitivity is not surprising; the fluorine-doped superconductor $Nd_2CuO_{4-x}F_x$ forms only in an extremely small window of oxygen partial pressure (*26*).

To conclude, the electrical and magnetic properties of the T* copper oxychlorides most closely resemble the properties of the T′ copper oxides, Ln_2CuO_4 (Ln = Nd, Sm) and not those of the $M_2CuO_2Cl_2$. Since several of the superconductors are doped Ln_2CuO_4 compounds, these T* copper oxides may become superconducting under proper conditions. The resistivity data on $CaSmCuO_3Cl$ and $Ca_{0.72}Sr_{0.28}NdCuO_3Cl$ suggest that a few divalent cations may be substituting into the Ln–O layer. Perhaps higher doping levels or annealing these compounds in high oxygen pressures will induce p-type superconductivity. We are presently pursuing such experiments.

Acknowledgments

The authors thank Dr. K. V. Ramanujachary, Dr. Shu Li, and Prof. Bill McCarroll for helpful discussions and Z. S. Teweldemedhin who aided with the magnetic susceptibility measurements. This work was supported by the Office of Naval Research and the National Science Foundation Grant DMR-87-14072.

References

1. F. Izumi, E. Takayama-Muromachi, A. Fujimori, T. Kamiyama, H. Asano, J. Akimitsu, and H. Sawa, *Physica C* **158,** 440 (1989).
2. Y. Tokura, H. Takagi, and S. Uchida, *Nature* **337,** 345 (1989).
3. G. M. Luke, B. J. Sternlieb, Y. J. Uemura, J. H. Brewer, R. Kadono, R. F. Kiefl, S. R. Kreitzman, T. M. Riseman, J. Gopalakrishnan, A. W. Sleight, M. A. Subramanian, S. Uchida, H. Takagi, and Y. Tokura, *Nature* **338,** 49 (1989).
4. G. Liang, J. Chen, M. Croft, K. V. Ramanujachary, M. Greenblatt, and M. Hedge, *Phys. Rev. B* **40,** 2646 (1989).
5. H. Müller-Buschbaum, *Angew. Chem. Int. Ed. Engl.* **16,** 674 (1977).
6. L. L. Miller, X. L. Wang, S. X. Wang, C. Stassis, D. C. Johnston, J. Faber, Jr., and C.-K. Loong, *Phys. Rev. B* **41,** 1921 (1990).
7. T. Sowa, M. Hiratani, and K. Miyauchi, *J. Solid State Chem.* **84,** 178 (1990).
8. J. G. Lee, unpublished results.
9. H. Sawa, S. Suzuki, M. Watanabe, H. Matsubara, H. Watabe, S. Uchida, K. Kokusho, H. Asano, F. Izumi, and E. Takayama-Muromachi, *Nature* **337,** 347 (1989).
10. E. Takayama-Muromachi, Y. Uchida, M. Kobayashi, and K. Kato, *Physica C* **158,** 449 (1989).
11. G. H. Kwei, R. B. Von Dreele, S-W. Cheong, Z. Fisk, and J. D. Thompson, *Phys. Rev. G* **41,** 1889 (1990).
12. L. H. Brixner, "Inorganic Syntheses" Vol. XIV, p. 126, McGraw Hill Co., New York (1973).
13. R. D. Shannon, *Acta Crystallogr. Sect. A* **32,** 751 (1976).
14. J. F. Bringley, S. S. Trail, and B. A. Scott, *J. Solid State Chem.* **86,** 310 (1990).
15. M. Tsai, M. Greenblatt, and W. H. McCarroll, *Chem. Mater.* **1,** 253 (1989).
16. F. Izumi, Y. Matsiui, H. Takagi, S. Uchida,

Y. TOKURA, AND H. ASANO, *Physica C***158,** 443 (1989).
17. C. S. SUNDAR, A. BHARATHI, Y. C. JEAN, P. H. HOR, R. L. MENG, Z. J. HUANG, AND C. W. CHU, *Phys. Rev. B* **42,** 426 (1990).
18. P. GANGULY AND C. N. R. RAO, *Mater. Res. Bull.* **8,** 405 (1973).
19. J. B. GOODENOUGH, *Mater. Res. Bull.* **8,** 423 (1973).
20. D. VAKNIN, S. K. SINHA, C. STASSIS, L. L. MILLER, AND D. C. JOHNSTON, *Phys. Rev. B* **41,** 1926 (1990).
21. Y. ENDOH, K. YAMADA, R. J. BIRGENEAU, D. R. GABBE, H. P. JENSSEN, M. A. KASTNER, C. J. PETERS, P. J. PICONE, T. R. THURSTON, J. M. TRANQUADA, G. SHIRANE, Y. HIDAKA, M. ODA, Y. ENOMOTO, M. SUZUKI, AND T. MURAKAMI, *Phys. Rev. B* **37,** 7443 (1988).
22. Y. ENDOH, M. MATSUDA, K. YAMADA, K. KAKURAI, Y. HIDAKA, G. SHIRANE, AND R. J. BIRGENEAU, *Phys. Rev. B* **40,** 7023 (1989).
23. R. SAEZ PUCHE, M. NORTON, T. R. WHITE, AND W. S. GLAUNSINGER, *J. Solid State Chem.* **50,** 281 (1983).
24. C. L. SEAMAN, N. Y. AYOUB, T. BJØRNHOLM, E. A. EARLY, S. GHAMATY, B. W. LEE, J. T. MARKERT, J. J. NEUMEIER, P. K. TSAI, AND M. B. MAPLE, *Physica C* **159,** 391 (1989).
25. M. KLAUDA, J. P. STRÖBEL, M. LIPPERT, G. SAEMANN-ISCHENKO, W. GERHAÜSER, AND H.-W. NEUMÜLLER, *Physica C* **165,** 251 (1990).
26. C. H. CHEN, D. J. WERDER, A. C. W. P. JAMES, D. W. MURPHY, S. ZAHURAK, R. M. FLEMING, B. BATLOGG, AND L. F. SCHNEEMEYER, *Physica C* **160,** 375 (1989).